



## INTERACTION BETWEEN ELEVATED CO<sub>2</sub> AND PHYTOPLANKTON-DERIVED ORGANIC MATTER UNDER SOLAR RADIATION ON BACTERIAL METABOLISM FROM COASTAL WATERS

5 Antonio Fuentes-Lema<sup>1</sup>; Henar Sanleón-Bartolomé<sup>2</sup>; Luis M. Lubián<sup>3</sup>; Cristina Sobrino<sup>1\*</sup>

<sup>1</sup> - UVigo Marine Research Centre; Lagoas Marcosende Campus 36331 Vigo, Spain

<sup>2</sup> - Spanish Institute of Oceanography (IEO). Paseo Marítimo Alcalde Francisco Vázquez 10,  
15001 A Coruña, Spain.

10 <sup>3</sup> - Institute of Marine Sciences of Andalucía (CSIC). Campus Univ. Rio San Pedro. 11519 Puerto Real,  
Cádiz, Spain

\*Correspondence to: Cristina Sobrino. +34 986 818789, [sobrinoc@uvigo.es](mailto:sobrinoc@uvigo.es)

Running head: Ocean acidification and DOM on bacteria

15

**Abstract.** Microcosm experiments to assess bacterioplankton response to phytoplankton-derived organic matter obtained under current and future-ocean CO<sub>2</sub> levels were performed. Surface seawater enriched with inorganic nutrients was bubbled for 8 days with air (current CO<sub>2</sub> scenario) or with a 1000 ppm CO<sub>2</sub>-air mixture (future CO<sub>2</sub> scenario) under solar radiation. The organic matter produced under the current  
20 and future CO<sub>2</sub> scenarios was subsequently used as inoculum. Triplicate 12 L flasks filled with 1.2 µm-filtered natural seawater enriched with the organic matter inocula were incubated in the dark for 8 days



under CO<sub>2</sub> conditions simulating current and future CO<sub>2</sub> scenarios to study the bacterial response. The acidification of the media increased bacterial respiration at the beginning of the experiment while the addition of the organic matter produced under future levels of CO<sub>2</sub> was related to changes in bacterial  
25 production and abundance. The balance between both, respiration and production, made that the bacteria grown under future CO<sub>2</sub> levels with an addition of non-acidified matter showed the best growth efficiency at the end of the incubation. However cells grown under future scenarios with high CO<sub>2</sub> levels and acidified organic matter additions did not perform differently than those grown under present CO<sub>2</sub> conditions, independently of the addition of acidified or non-acidified organic matter. This study  
30 demonstrates that the increase in atmospheric CO<sub>2</sub> concentrations can affect bacterioplankton directly by changes in the respiration rate and indirectly by changes on the organic matter with concomitant effects on bacterial production and abundance.

**KEY WORDS:** bacterioplankton, phytoplankton, organic matter, ocean acidification.



## 35 **1 Introduction:**

The increase in fossil fuel burning, cement production and deforestation together with changes in land use have resulted in an accumulation of atmospheric CO<sub>2</sub> at levels never seen before the last two million years (Caldeira & Wickett 2008, Le Quere et al. 2015). Atmospheric gases can freely diffuse into the ocean surface, which has already absorbed about 30% of the emitted anthropogenic CO<sub>2</sub>, perturbing the carbonate system and decreasing ocean pH in a process known as ocean acidification (Sabine et al. 2004, 40 Burke et al. 2014).

The latest IPCC report shows that the pH of surface ocean waters has already decreased by 0.1, corresponding to a 26% increase in acidity. If mitigation strategies for global change are not adopted and CO<sub>2</sub> emissions continue as usual, ocean pH values will drop about 0.3-0.7 units by the end of the 21<sup>st</sup> 45 century (Burke et al. 2014). The decrease in seawater pH has strong effects on the ecosystem, the aquatic organisms and the interactions among them. Studies about its consequences in the surface ocean have been primarily focused on calcifying organisms such as corals or coralline algae because they participate in the formation of habitats and human services (Langdon et al. 2003, Fabry et al. 2008). Recent meta-analysis studies also revealed decreased survival, growth, development and abundance of a broad range 50 of marine organisms, although the magnitude of these responses varies between taxonomic groups, including variation within similar species (Kroeker et al. 2013). Additionally, other authors have demonstrated that ocean acidification can increase growth, primary production and N<sub>2</sub> fixation rates in some phytoplankton species (Barcelos e Ramos et al. 2007, Fu et al. 2007, Levitan et al. 2007, Iglesias-Rodriguez et al. 2008). In contrast with the abundant information about phytoplankton, very little is 55 known about the response of their heterotrophic counterparts.



Heterotrophic bacteria play an important role in the planktonic community since they are responsible for the majority of the organic matter remineralization (Cole et al. 1988, Azam et al. 1998, Nagata et al. 2000) allowing the primary producers to make use of the recycled inorganic nutrients. They also return dissolved organic carbon (DOC) to the marine food web via its incorporation into bacterial biomass through what it is called the microbial loop (Azam et al. 1983). The other way around, the microbial response can change depending on phytoplankton taxonomic composition and the nutrient levels, and therefore productivity, of the water (Teira et al. 2012, Bunse et al. 2016, Sala et al. 2016). Despite this important role of bacterioplankton in the marine food web and biogeochemical cycles, only few studies have been designed to elucidate the effects of ocean acidification on bacteria metabolism or its interaction with the abiotic or biotic factors. Some of these studies suggest an absence of significant metabolic responses in experiments where CO<sub>2</sub> levels were manipulated (Rochelle-Newall et al. 2004, Allgaier et al. 2008, Newbold et al. 2012). Adaptation towards a fast acclimation to low pH values might have occurred since occasionally bacteria and other heterotrophic organisms, suffer lower pH values than those predicted by ocean acidification scenarios (Joint et al. 2011). On the contrary, other authors have reported that a decrease in seawater pH can potentially influence bacterial metabolism by changes in bacterial production and growth rates in natural communities, although the results show different responses depending on the study (Coffin et al. 2004, Grossart et al. 2006, Motegi et al. 2013, Spilling et al. 2016). More recently, results from a phytoplankton bloom mesocosm study have demonstrated, through metatranscriptome analysis, that acidification can enhance the expression of genes encoding proton pumps to maintain homeostasis under high CO<sub>2</sub> conditions (Bunse et al. 2016).



An interesting point is that the experimental design in most of the published CO<sub>2</sub> studies did not allow distinguishing between direct effects on the bacteria *per se* and indirect effects, due for example to changes in phytoplankton community composition or to changes in organic matter. Therefore, indirect pathways such as those affecting the availability of organic matter in terms of quantity, because of an increase in phytoplankton primary production (Hein & Sand-Jensen 1997, Riebesell et al. 2007), or in terms of quality, because of changes in the composition of phytoplankton-derived organic matter (Engel et al. 2014), should be also studied to determine the effect of ocean acidification on bacterioplankton. For example, recent results have demonstrated that pH values predicted for future ocean acidification scenarios were close to the optimum values for extracellular enzyme activity (Grossart et al. 2006, Piontek et al. 2010, Yamada & Suzumura 2010). Higher enzymatic activity resulted in a higher rate of organic matter transformation and increases in bacteria performance. It has been also demonstrated that decreases in pH might increase the rate of extracellular dissolved organic carbon production from phytoplankton (DOC<sub>p</sub>) and the formation of transparent exopolymer particles (TEPs) (Engel 2002, Engel et al. 2004), although the contrary has also been observed and there is not a clear response to this matter (Sobrino et al. 2014). In addition, a higher CO<sub>2</sub> concentration in seawater could modify the C:N:P ratios of particulate organic matter, which may substantially affect the activity of bacteria and the carbon fluxes in the future ocean (Riebesell et al. 2007, Engel et al. 2014).

Environmental drivers such as the ultraviolet radiation (UV: 280-400 nm) should be also taken into account when studying the biological and chemical responses of the planktonic assemblages and the environment, since it plays a crucial role on the physiology of plankton communities and on the ecology of the aquatic ecosystems. UVR induces photomineralization of coloured dissolved organic matter



(CDOM) increasing the biological availability of the resulting DOM (Moran & Zepp 1997). UV radiation can also increase DOC<sub>p</sub> production in surface waters (Carrillo et al. 2002, Helbling et al. 2013, Fuentes-Lema et al. 2015).

100 The main goal of our study was to investigate the direct and indirect effects of ocean acidification on the interaction between phytoplankton derived organic matter and bacterial metabolism. We analyzed the changes in bacterial abundance, production, respiration and viability in a coastal plankton community from an upwelling system subjected to current and future CO<sub>2</sub> concentrations.

## 105 **2 Materials and Methods:**

### *2.1 Experimental Setup*

The experiment to determine the response of bacterioplankton communities to phytoplankton-derived organic matter produced under current and future CO<sub>2</sub> scenarios were performed in two phases at the Toralla Marine Science Station, from now on ECIMAT (Estación de Ciencias Mariñas de Toralla, University of Vigo ([ecimat.uvigo.es](http://ecimat.uvigo.es))) (Fig. 1). The first phase consisted in 8 days incubation under full solar radiation (UV radiation included) of natural phytoplankton communities enriched with inorganic nutrients under current and future CO<sub>2</sub> conditions. In the second phase, the organic matter obtained from the previous incubation was added to a natural bacterioplankton community to assess the interactions between organic matter amendments and acidification on bacterial metabolism for 8 days (Fig. 2).

115 Water from 5 m depth was collected with a Niskin bottle on board of the R/V Mytilus from a fixed central station at the Ría de Vigo (42.23 N; Long: 8.78 W. Fig. 1) the 27<sup>th</sup> of June 2013 and immediately transported to the ECIMAT (approx. 30 min). The Ría de Vigo is a highly productive and dynamic



embayment located in the Northwestern Iberian Peninsula, characterized by the intermittent upwelling of cold and inorganic nutrient-rich Eastern North Atlantic Central water (Fraga 1981). Upwelled water in the Iberian system also brings high CO<sub>2</sub> concentrations, so annual *p*CO<sub>2</sub> can oscillate between maximum values of 750 ppm CO<sub>2</sub> during the upwelling events and minimum values of 270 ppm CO<sub>2</sub> during the downwelling season (Alvarez et al. 1999, Gago et al. 2003). The sample was pre-screened using a 200 µm sieve to avoid zooplankton grazing and distributed in six, aged and acid washed, UVR transparent 20 L cubitainers (NalgeneR I-Chem Certified Series™ 300 LDPE Cubitainers). The cubitainers were submerged in two 1500 L tanks located outdoors in an open area free of shadows. The tanks were connected to a continuous seawater pumping system and covered by a neutral density screen (75% Transmittance) to assure cooling at the *in situ* temperature and to avoid photoinhibition by the highly damaging summer irradiances under the static conditions of the cubitainers, respectively. Nitrate, ammonium and phosphate were added the first and 5<sup>th</sup> day of experiment to maintain saturating nutrient conditions (5 µmol L<sup>-1</sup> nitrate (NO<sub>3</sub><sup>-</sup>), 5 µmol L<sup>-1</sup> ammonium (NH<sub>4</sub><sup>+</sup>) and 1 µmol L<sup>-1</sup> phosphate (HPO<sub>4</sub><sup>-2</sup>) final concentrations). Triplicate samples were bubbled with regular atmospheric air (Low Carbon treatment: LC, aprox. 380 ppm CO<sub>2</sub>) or with a mixture of the atmospheric air and CO<sub>2</sub> from a gas tank (Air Liquide Spain) (High Carbon treatment: HC, 1000 ppm CO<sub>2</sub>). At the end of the incubation, the samples grown under present and future levels of CO<sub>2</sub> were stored frozen at -20 °C until the start of the second phase, ten days later, to be used as a naturally-derived organic matter inocula. The inocula included both, dissolved and particulate organic matter, as observed in nature, but since bacteria preferentially use the labile dissolved organic matter pool for growth (Nagata et al. 2000, Lechtenfeld et al. 2015) we focused our measurements of the organic matter on the dissolved fraction.



For the second phase, water collection was similar to the previous one. Once at ECIMAT, seawater was  
140 filtered through 1.2  $\mu\text{m}$  pore size glass fiber filters (GF/C Whatman Filters) to separate the  
bacterioplankton community from the other plankton cells, mainly diatoms for this time of the year  
(Tilstone et al. 2000, Fuentes-Lema & Sobrino 2010). The bacterioplankton sample was distributed in 12  
acid washed polycarbonate NALGENE 12 L bottles together with the phytoplankton derived organic  
matter inoculum and 0.2  $\mu\text{m}$  filtered seawater (FSW) following a 3:1:6 bacterioplankton: organic matter:  
145 FSW volume ratio, respectively. This proportion aimed to reach 10  $\mu\text{mol L}^{-1}$  of organic carbon, which  
represent around 25-30% of the mean excess of organic carbon observed in the surface layer of the middle  
Ría de Vigo as compared with the bottom waters (Doval et al. 1997, Nieto-Cid et al. 2005). Half of the  
bottles were inoculated with organic matter produced under current  $\text{CO}_2$  conditions (Non acidified  
Organic matter, NO, n=6) and the other half with organic matter produced under future  $\text{CO}_2$  conditions  
150 (Acidified Organic matter, AO, n=6). In each case, three replicates were aerated with ambient  $\text{CO}_2$  levels  
(Low Carbon treatment (LC): LC\_NO, LC\_AO) or air with 1000 ppm  $\text{CO}_2$  (High Carbon treatment (HC):  
HC\_NO, HC\_AO). This experimental setup produced 4 different treatments from the less modified  
sample (LC\_NO) to the most altered sample (HC\_AO) (Fig. 2). The bottles were located in a walk-in  
growth chamber under dark conditions at 15  $^\circ\text{C}$ , similar to *in situ* temperatures, with the aim of focusing  
155 the experiment on the two factors of the study, avoiding potential photoinhibitory and photochemical  
effects of solar radiation on bacterioplankton and organic matter, respectively.

## 2.2 DIC, pH and $\text{CO}_2$ analysis





160 Triplicate 30 mL samples were filtered daily through 0.2  $\mu\text{m}$  size pore nitrocellulose filters. The filtrate  
was encapsulated without air bubbles in 10 mL serum vials and stored at 4 °C and dark conditions until  
analysis immediately after the incubation ended. Dissolved Inorganic Carbon (DIC) analysis was carried  
out through acidification with 10% HCl using a N<sub>2</sub> bubbler connected to an infrared gas analyzer (LICOR  
7000) and calibration was performed using a Na<sub>2</sub>CO<sub>3</sub> standard curve. pH and temperature were daily  
measured with a Crison pH 25 pH meter and salinity with a thermosalinometer Pioneer 30. The pH meter  
165 was calibrated to the total hydrogen ion concentration pH scale with a 2-amino-2-hydroxymethyl-1,3-  
propanediol (tris) buffer prepared in synthetic seawater (Dickson & Goyet 1994). The partial pressure of  
CO<sub>2</sub> ( $p\text{CO}_2$ ) in the samples was calculated from salinity, temperature, pH and DIC using the software  
csys.m from Zeebe & Wolf-Gladrow (2001).

### 170 2.3 *Chlorophyll a* concentration

Seawater samples for Chl *a* analysis were taken every day during the first incubation. A volume of 150  
mL from each cubitainer was gently filtered through GF/F filters under dim light and immediately stored  
at -20 °C until further analysis. For Chl *a* extraction, the filters were kept at 4 °C overnight in acetone  
90%. Chl *a* concentration was estimated with a Turner Design Fluorometer TD-700 and a pure Chl *a*  
175 standard solution was used for calibration.

### 2.4 *Primary production*

Incubations were performed at noon and lasted 3 to 3.5 hours. Fifteen mL samples of each microcosm  
were inoculated with H<sup>14</sup>CO<sub>3</sub> (approximately 1  $\mu\text{Ci mL}^{-1}$  final concentration) and incubated in UVR



180 transparent Teflon-FEP bottles under full solar radiation exposures in a refrigerated tank contiguous to  
the experimental microcosms. The teflon bottles were tied on top of a UVR transparent acrylic tray,  
keeping all bottles under flat and constant position. Tray was wrapped with 2 layers of neutral density  
screen to obtain saturating but non-photoinhibitory solar exposures. For analysis of the fraction of the  
fixed carbon incorporated into particulate (POC) and dissolved (DOC) organic carbon, 5 mL samples  
185 were filtered through 0.2  $\mu\text{m}$  PC filters (25 mm diameter) under low pressure (50 mm Hg) after the light  
incubation period, using 2 manifolds simultaneously (10 positions per manifold). POC was retained on  
the filter while the filtrate was directly collected in scintillation vials to assess  $^{14}\text{C}$  activity in the dissolved  
fraction (DOC). Simultaneously, the total amount of organic carbon incorporated in the cells (TOC) was  
measured independently of the DOC-POC filtration by processing 5 mL of the incubated samples. Non-  
190 assimilated  $^{14}\text{C}$  was released by exposing the filters (POC) to acid fumes (50% HCl) or by adding 200  $\mu\text{l}$   
of 10% HCl to the liquid samples (DOC & TOC, respectively) and shaking overnight. The radioactivity  
of each sample was measured using a Wallac WinSpectral 1414 scintillation counter (EG&G Company,  
Finland). There was no significant difference between measurements of TOC compared to the sum of the  
particulate and dissolved fractions ( $R^2=0.94$ ,  $n=12$ ).

195

### *2.5 Bacterial production and respiration*

Bacterial production (BP) was measured following the [ $^3\text{H}$ ] leucine incorporation method (Smith & Azam  
1992). Three replicates and 1 killed control were sampled (1 mL) from each experimental unit on days 0,  
1, 2, 3, 4 and 7 of the second incubation. Samples were spiked with 40  $\mu\text{L}$  Leucine (47  $\mu\text{Ci mL}^{-1}$  specific  
200 activity stock solution), and incubated for 80 min in the same chamber and growth conditions than the



bacterioplankton assemblages. Processed samples were analyzed in a Wallac Win-Spectral 1414 scintillation counter and the BP was calculated from the Leucine uptake rates employing the theoretical leucine to carbon conversion factor ( $3.1 \text{ kg C mol Leu}^{-1}$ ) (Simon & Azam 1989).

205 Samples for bacterial respiration (BR) were taken on days 0, 2, 4 and 7 of the second incubation. BR in each sample was determined from the difference of the dissolved oxygen concentration consumed between the end and the start of a 24 h dark incubation using 50 mL Winkler bottles in duplicate. The 24 h incubation was carried out at the same temperature than the experiment. Dissolved oxygen concentrations were determined by automated high-precision Winkler titration, using a potentiometric end point detector, Metrohm 721 DMS Titrino, as described in Serret et al. (1999). Bacterial carbon  
210 demand (BCD) was calculated as the sum of BP and BR. Bacterial growth efficiency (BGE) was obtained from the proportion of the BCD that was used for bacterial production ( $\text{BGE} = \text{BCD}/\text{BP}$ ).

### 2.6 Flow cytometry analysis

For phytoplankton (i.e. first incubation), samples were collected, fixed with P+G (1% paraformaldehyde  
215 + 0.05% glutaraldehyde) and analyzed with a FACScalibur flow cytometer (Becton–Dickinson). Measurements of the different photodetectors were made with a logarithmic amplification for each signal, and the trigger was set on red fluorescence (FL3). Phytoplankton counts were obtained at a high flow rate ( $1.05 \mu\text{L s}^{-1}$ ) during 10 min. Two size groups of cells (R1 and R2) were discriminated on the bivariate plots of side light scatter (SSC) vs. FL3.

220 For bacterioplankton counts (i.e. second incubation), samples were stained with  $2.5 \mu\text{M}$  of SYTO-13 (Molecular Probes) dissolved in dimethyl sulfoxide. The samples were incubated during 10 min at room



temperature in the dark, followed by the addition of 10  $\mu\text{L}$  of a microspheres solution (FluoSpheres  
carboxylated-modified microspheres (1.0  $\mu\text{m}$  nominal diameter). ThermoFisher Scientific) as internal  
standard for instrument performance. Samples were then immediately analyzed. The threshold was set on  
225 the green fluorescence (FL1). Stained bacteria were discriminated and counted in a bivariate plot of SSC  
vs. FL1.

Viability of bacterioplankton community was measured on day 7 using the 5-Cyano-2,3-ditolyl  
tetrazolium chloride (CTC) dye (Sieracki et al. 1999; Gasol and Arístegui 2007). The CTC can freely  
diffuse into the cells where it is reduced by healthy respiring bacteria, producing a precipitated colored  
230 red/orange formazan product. This product is detectable and quantifiable by flow cytometry (Rodriguez  
et al. 1992). Samples were stained with 45 mM of CTC during 60 minutes and then analyzed. Threshold  
was set on the FL3 and viable bacteria were counted in a bivariate plot of SSC vs. FL3.

All data were acquired and analyzed with the software CellQuest (Becton– Dickinson) as Flow Cytometry  
Standard files.

235

### *2.7 DOC concentration*

Dissolved organic carbon samples were taken in 250 mL acid-washed all-glass flasks and were gently  
filtered through acid rinsed 0.2  $\mu\text{m}$  Pall-Supor filters. All this process was done in an acid-cleaned all-  
glass device under low  $\text{N}_2$  flow pressure. About 10 mL of the filtrates were distributed in pre-combusted  
240 (450  $^\circ\text{C}$  for 24 h) glass ampoules acidified with 50  $\mu\text{L}$  of 25%  $\text{H}_3\text{PO}_4$ . The ampoules were heat sealed  
immediately and stored at 4  $^\circ\text{C}$  until analysis with a Shimadzu TOC-VCS analyzer following the high  
temperature catalytic oxidation method (Álvarez-Salgado & Miller 1998).



## 2.8 Statistical analysis

245 When the data followed a normal distribution and homoscedasticity, tested by Lilliefors test, a one way-ANOVA and multiple comparison post-test (MCP-test) or *t*-Test were employed to determine differences among the mean of several or paired samples, respectively. In the case that data did not follow a normal distribution, a non-parametric repeated-measures ANOVA (RMANOVA) and a Tukey-Kramer multiple comparison post-test were chosen. The Wilcoxon signed rank test was used to compare non-parametric  
250 paired samples. The confidence level was established at the 95%. Statistical analysis was performed using the software packages MatLab R2012b and GraphPad InStat TM v2.04a+.

## 3 Results:

During the first incubation, aimed to obtain the organic matter inocula under current and future CO<sub>2</sub>  
255 conditions, the LC treatment *p*CO<sub>2</sub> values were close to the atmospheric equilibrium, with values ranging between 419 ± 21 ppm CO<sub>2</sub> on day 0 and 226 ± 38 ppm CO<sub>2</sub> on day 3 (mean and SD, n=3) (Fig. 3A). In the HC treatment *p*CO<sub>2</sub> values increased since the beginning of the incubation until reaching values around 1200 ppm the last four days. Maximum values were observed at day 5 with 1227 ± 149 ppm CO<sub>2</sub>. Chl *a* used as an indicator of the phytoplankton biomass showed similar trends in the two treatments. It  
260 increased with the initial addition of inorganic nutrients showing an early bloom on day 1 with Chl *a* values of 21 ± 4 µg L<sup>-1</sup> and 22 ± 9 µg L<sup>-1</sup> for LC and HC treatments, respectively. Chl *a* concentration decreased after the bloom, keeping values close to the lowest concentrations on day 6 for the HC treatment with 3.0 ± 0.4 µg L<sup>-1</sup> and on day 5 for the LC treatment, 3.1 ± 0.5 µg L<sup>-1</sup> (Fig. 3A).



Flow cytometry results showed a succession of two different phytoplankton populations along the incubation characterized by differences in cell size and Chl content (Table 1). In both treatments, larger cells with higher Chl *a* fluorescence and cell complexity (Region 1, Table 4.2.1), dominated the phytoplankton community at the beginning of the incubation. The abundance of these large cells decreased, especially in the HC treatment, and at the end of the incubation smaller cells, with lower Chl content became more abundant (Region 2, Table 4.2.1). At day 7 the small size fraction population was dominant and the analyzed phytoplankton community was similar in both, HC and LC treatments.

Primary production rates followed the Chl *a* pattern with a marked peak blooming the first incubation day followed by a decline afterwards in all the treatments (Fig. 4). The increase in total carbon fixation during the bloom was due to an increase in both, DOC and POC production, but it was mainly due to POC assimilation. The percentage of extracellular release of dissolved carbon ( $PER = DOC / (POC + DOC)$ ) ranged between 18% and 77%. DOC, POC, and therefore TOC, were higher during the bloom under the LC treatment but not significantly different than the rates observed in the HC treatment. Differences in the production rates between both treatments became negligible after the second incubation day (Fig. 4). DOC concentration increased from day 0 to maximum values on day 7, and similar to Chl *a* concentration, production rates and cell abundance, there were not significant differences between the two CO<sub>2</sub> treatments at the end of the incubation (Fig. 3B). Parallel analysis of DOM fluorescence (*i.e.* protein-like and humic-like substances) also supported the later results (data not shown).

In the second incubation, aimed to assess the effects of CO<sub>2</sub> and the organic matter additions on bacterioplankton, *p*CO<sub>2</sub> and pH were similar within the same CO<sub>2</sub> treatment (*i.e.* LC\_NO and LC\_AO vs. HC\_NO and HC\_AO), but significantly different between LC and HC treatments (Fig. 5A and B). *p*CO<sub>2</sub>



285 in the LC ranged between  $350 \pm 28$  ppm and  $568 \pm 187$  ppm  $\text{CO}_2$  (mean and SD,  $n=3$ ) on day 5 and 2, respectively. In contrast, HC treatments increased from  $397 \pm 18$  ppm on day 0 to a maximum value of  $2213 \pm 229$  ppm on day 3, significantly different that the expected 1000 ppm  $p\text{CO}_2$  in the HC treatments. The maximum was followed by a pronounced decrease on day 4, and subsequently, the values were similar to the bubbled air concentrations ( $1011 \pm 75$  ppm on day 5) (Fig. 5A). As expected from the  $p\text{CO}_2$ ,  
290 pH values in the LC treatments were fairly constant with a mean value of 8.07 but decreased markedly from 8.03 on day 0 to 7.51 on day 3 in the HC treatment. After this minimum, pH increased to values around 7.8 until the end of the experiment (Fig. 5B).

The changes in  $\text{CO}_2$  concentration and pH were concomitant with an increase in BR in the HC treatments (Fig. 5C). BR was also fairly constant in the LC treatments, but increased significantly from day 0 to day  
295 2 in the HC treatments. After reaching the maximum, bacterial respiration dropped to similar values than those observed in the LC treatments (Fig. 5C). Among them the LC\_NO treatment showed the lowest variability in the respiration rates and the highest values at the end of the incubation. Similar to  $p\text{CO}_2$  and pH, statistical differences between samples with inocula produced under current and future  $\text{CO}_2$  scenarios within each  $\text{CO}_2$  treatment were not significant regarding respiration rates. Flow cytometry analysis of  
300 the bacteria viability using the CTC dye, which has been previously related to the respiration rates, showed that the LC\_NO treatment had significantly higher values than the other treatments on day 7 (RMANOVA and Tukey-Kramer MCT,  $p<0.05$ ). In contrast, the other three treatments did not show significant differences among them (Fig. 6)

The initial concentration of dissolved organic carbon (DOC,  $\mu\text{M-C}$ ) in the samples was quite similar  
305 among the four treatments until the peak in respiration. DOC before the addition of the organic matter



inocula was  $89 \mu\text{M-C}$  and increased in all the treatments to maximum values of  $111 \pm 5 \mu\text{M-C}$  and  $117 \pm$   
n.d.  $\mu\text{M-C}$  in treatments LC\_AO and HC\_NO on day 3, respectively. Afterwards DOC in the LC  
treatments kept approximately constant but decreased 27% in the HC treatments compared to the LC  
treatments ( $81 \pm 3 \mu\text{M-C}$  and  $81 \pm 2 \mu\text{M-C}$  in HC\_NO and HC\_AO, respectively). Statistical analysis  
310 showed significant differences between both  $p\text{CO}_2$  treatments on day 7 (ANOVA and  $t$ -Test for paired  
treatments,  $p < 0.01$ ) (Fig. 7).

Unlike  $p\text{CO}_2$ , pH, respiration and DOC, bacterial abundance and production showed differences regarding  
the origin of the organic matter. The addition of the organic matter inocula produced a fast increase in  
production and abundance from day 0 to day 3 in all the treatments. Cell abundance increased from  $6.2 \pm$   
315  $0.4 \times 10^4$  bacteria  $\text{mL}^{-1}$  before the addition of the organic matter inocula to a maximum of  $9.0 \pm 0.4 \times 10^5$   
bacteria  $\text{mL}^{-1}$  in the HC\_AO treatment (Fig. 8A). Differences for the bacterial abundance started to be  
significant in day 1 but they were more clearly observed during the maximum at day 3 (ANOVA and  
MCP-test,  $p < 0.05$ ). Bacterial abundances were 29% and 31% higher in samples where the acidified  
organic matter was added than in those with the addition of organic matter produced under the current  
320  $\text{CO}_2$  scenario, in the LC and HC treatments, respectively (Fig. 8A).

Additionally, bacterial production increased from a minimum value of  $1.1 \pm 0.1 \mu\text{g C L}^{-1} \text{d}^{-1}$  on day 0 to  
maximum values on day 2 for the four treatments, ranging between  $185 \pm 37 \mu\text{g C L}^{-1} \text{d}^{-1}$  and  $208 \pm 4 \mu\text{g}$   
 $\text{C L}^{-1} \text{d}^{-1}$  for HC\_NO and LC\_NO, respectively. From the maximum values at day 2 to the end of the  
incubation, the treatments with the addition of acidified organic matter (LC\_AO and HC\_AO) showed a  
325 higher decrease in the production rates than those with the addition of the non-acidified organic matter,





resulting in significant differences later on. On day 7 treatments LC\_NO and HC\_NO produced 53% and 45% more than treatments LC\_AO and HC\_AO, respectively (Fig. 8B).

The BCD was biased by the respiratory activity at the beginning of the incubation and by the production at the end, showing the treatments with the addition on non-acidified organic matter significantly higher carbon demand than the treatments with the addition of acidified organic matter at day 7 (ANOVA and MCP-test,  $p < 0.05$ ) (Fig 9A). In consequence, the BGE was higher for the LC treatments, at the beginning of the incubation during the activity peak, but decreased at the end. At day 7 the HC treatment with the addition of non-acidified organic matter (HC\_NO) showed significantly higher efficiency than the other treatments (ANOVA and MCP-test,  $p < 0.05$ ) (Fig 9B). Conversely, the HC\_AO treatment expected for future scenarios of global change did not show significant differences with neither of the LC treatments.

#### 4 Discussion:

The main goal of the current study was to distinguish between the direct and indirect effects of ocean acidification on natural bacterial assemblages. To achieve this objective we performed a 2×2 experimental design combining the acidification of seawater and the addition of phytoplankton-derived organic matter produced under current and future CO<sub>2</sub> conditions and natural solar exposures. Although there have been described different ways to modify the seawater pH to simulate an ocean acidification scenario, the continuous bubbling of the natural plankton communities with a target CO<sub>2</sub> concentration of 1000 ppm CO<sub>2</sub> was chosen in the present study to simulate the  $p\text{CO}_2$  and pH conditions expected for the end of the century. This method ensures quite realistic responses in terms of acclimation rates (Rost et al. 2008). It also allows that changes in the biological activity of the samples enable the modification of the  $p\text{CO}_2$



values if, for example, the photosynthetic or respiratory rates become faster than the rates needed to achieve the CO<sub>2</sub> chemical equilibrium in seawater. Changes in *p*CO<sub>2</sub> values due to microbial activity are usually observed in natural waters during bloom events in surface waters or in areas with high amount of  
350 organic matter (Joint et al. 2011). *p*CO<sub>2</sub> also increases with depth due to the increase in heterotrophic activity compared to the autotrophic activity in surface (Pukate & Rim-Rukeh 2008, Dore et al. 2009) and can change due to upwelling events, for example in the same area where the samples were collected, reaching values close to those observed in the present work (Alvarez et al. 1999, Gago et al. 2003).

In our study, the CO<sub>2</sub> enrichment did not produce a significant effect on phytoplankton production or  
355 biomass, measured as <sup>14</sup>C incorporation or Chl *a* concentration, respectively. Phytoplankton community composition changed from bigger to smaller phytoplankton cells, as has been observed in similar microcosm studies (Reul et al. 2014, Grear et al. 2017), but differences between present and future CO<sub>2</sub> treatments were not observed. DOC<sub>p</sub> production increased during the bloom evolved at the beginning of the incubation but bulk DOC concentration showed similar values between CO<sub>2</sub> treatments, as expected  
360 based on the lack of differences observed in the biological and metabolic parameters. Despite several studies indicate an increase in phytoplankton carbon production and biomass under future scenarios of CO<sub>2</sub> (Kroeker et al. 2013), in our study exposure of the cells to natural conditions including solar UVR might have counteracted the stimulatory effect of the high CO<sub>2</sub>, since it increases the sensitivity of phytoplankton to photoinhibition (Sobrino et al. 2008, 2009, Gao et al. 2012).

365 The addition of the organic matter and the start of the aeration in the second incubation produced a burst in the metabolic activity of the bacteria. Bacterioplankton growing in the HC treatments showed higher rates of respiration the first two days. This response was opposite to that described for some bacterial



cultures (Teira et al. 2012) and seems to be related to an acclimation to the new pH values, somehow similar to observed for phytoplankton (Sobrino et al. 2008). Consequently,  $p\text{CO}_2$  in the HC treatments  
370 increased more than expected due to the biological activity carried out by bacterioplankton. The increase in respiration was also concomitant to an increase in bacterial abundance and production. However, the results indicate that while changes in respiration were related to  $p\text{CO}_2$  values, changes in bacterial abundance and production were mainly related to the origin of the organic matter amendments. The bacterial abundance was stimulated by the presence of organic matter from a phytoplankton community  
375 grown under high  $\text{CO}_2$  conditions compared to the addition of organic matter values grown under current  $\text{CO}_2$  conditions, at the beginning of the incubation (up to day 3). On the other hand, differences in bacterial production were only significant at the end of the experiment (day 7).

Possible explanations for the preference of the organic matter produced under future  $\text{CO}_2$  conditions by bacteria are changes in the composition and quality of this organic matter, changes in the capability of  
380 bacteria to use this organic matter via extracellular enzymatic activity or a combination of both. Several mesocosm studies have shown that the rate of extracellular release of phytoplankton dissolved organic matter production and the formation of transparent exopolymer particles (TEPs) is higher under high  $\text{CO}_2$  conditions (Engel 2002, Liu et al. 2010, Endres et al. 2014). TEPs are mostly carbon rich, can be easily consumed by heterotrophic bacteria and can aggregate and coagulate in larger gel-like structures that  
385 provide nutrients and attachment surface to bacteria, finally acting as hotspots where bacteria can grow and develop (Azam & Malfatti 2007). However, our results from the initial incubation aimed to obtain phytoplankton-derived organic matter inocula for bacteria do not suggest differences on DOC concentration under current and future  $\text{CO}_2$  conditions (Fig. 3B), and neither composition, since



phytoplankton community and fluorescence DOM properties were similar in both treatments at the end  
390 of the experiment (Table 1). Recent results from mesocosm experiments showing no significant  
differences in DOM concentration and composition between current and future CO<sub>2</sub> levels also  
corroborate these findings (Zark et al. 2015). Other than this, very little was found in the literature about  
the direct impact of ocean acidification on the DOM pool, particularly on its molecular composition and  
long-term reactivity.

395 Despite the significant effect on bacterial abundance during the activity peak, bacterial production only  
showed significant differences among treatments later during the incubation, having bacteria inoculated  
with the organic matter produced under high CO<sub>2</sub> conditions lower production rates than those with the  
organic matter produced under low CO<sub>2</sub> conditions. These results support a higher bioavailability of the  
organic matter produced under high CO<sub>2</sub> conditions to bacteria earlier during the incubation, increasing  
400 bacterial abundance, and decreasing production later at the end of the experiment. The lower DOC values  
in the HC treatments at the end of the experiment compared to the LC treatments partially supports this  
contention in the HC\_AO treatment. However, they mainly indicate a clear effect of the pH,  
independently of the origin of the organic matter inocula. We hypothesized that low pH, directly or  
indirectly, could be responsible for a faster and more efficient degradation of the most recalcitrant organic  
405 carbon, also in the HC\_NO, at the end of the experiment. On one hand, the lower DOC in the HC  
treatments compared to the LC treatments at the end of the experiment could be an indirect consequence  
of the higher respiration rates, which lowered the pH values (i.e. *p*CO<sub>2</sub> values above the expected 1000  
ppm) in these treatments during the activity peak. Between the two incubation performed for this study,  
the significant effect of the pH on the DOC content might have been only observed in the second



410 incubation because it reached almost double de  $p\text{CO}_2$  than the first one (i.e. min pH= 7.48 for the bacterioplankton incubation vs. min pH= 7.71 for the phytoplankton incubation). Following this contention, if acidification increases the degradation rate and bioavailability of the organic matter, that would explain why respiration in the control treatment (LC\_NO) was only significantly higher at the end of the experiment, where neither the organic carbon added nor the environment were modified by the  
415 acidification with  $\text{CO}_2$ . Flow cytometry results confirmed the highest rates of respiration in the LC\_NO treatment since the CTC dye is reduced to a quantifiable fluorescent CTC-formazan inside cells when the electron transport system is active (Sieracki et al. 1999, Gasol & Arístegui 2007).

On the other hand, previous studies have confirmed that many enzymes involved in the hydrolysis of organic matter are sensitive to pH variations. It has been reported that important enzymes for bacterial  
420 metabolism such as leucine aminopeptidase or the  $\alpha$ - and  $\beta$ -glucosidase enhance their activity and transformation rates with small decreases in pH, similar to the values measured in this study (Grossart et al. 2006, Piontek et al. 2010, 2013). The effects of ocean acidification on enzyme activity is not constant and could vary depending on enzyme type and geographical location (Yamada & Suzumura 2010). Despite our results show that the increase in bacterial abundance is mainly related to the presence of  
425 organic matter produced under future  $\text{CO}_2$  conditions and not so much to the decrease in pH, a trend that supports a synergistic effect of both, acidified organic matter and pH, can be observed. This trend shows the highest effects under the most extreme HC\_AO treatment and the lowest effects under the less aggressive LC\_NO treatment (i.e. for bacterial abundance the 3<sup>rd</sup> day of incubation and partially for production and viability on day 7). It can be also possible that enhanced extracellular enzymes produced  
430 by the microbial community under high carbon conditions during the first incubation aimed to obtain the



organic matter inocula came with the acidified organic matter since there is evidence that  $\beta$ -glucosidase, leucine aminopeptidase, and phosphatase enzymes are stable in cold waters for weeks (Steen & Arnosti 2011).

The uncoupling between pH and organic matter effects on bacterial respiration and production made that  
435 the carbon demand was biased by the most significant effect along the incubation. Therefore the least  
perturbed treatment with cells grown under present CO<sub>2</sub> conditions and non acidified organic mater (i.e.  
LC\_NO) showed the highest growth efficiency after the organic matter addition, during the activity peak,  
because of the lack of pH changes and lower respiration rates. However, after 7 days an intermediate  
treatment with high CO<sub>2</sub> levels but non-acidified organic matter addition (i.e. HC\_NO) had the highest  
440 growth efficiency due to the higher production rates and the relatively lower respiration rates compared  
to the treatment grown under current conditions but addition of non-acidified organic matter (LC\_NO).  
Cells grown under future scenarios with high CO<sub>2</sub> levels and acidified organic matter additions did not  
perform differently than those grown under present CO<sub>2</sub> conditions, independently of the addition of  
acidified or non-acidified organic matter. BGE and bacterial abundance did agree at the end of the  
445 experiment showing the HC\_NO treatment the highest cell abundance, although without significant  
differences among treatments. Nonetheless, further studies are needed to disentangle the lack of  
agreement among bacterial production, abundance and growth efficiency, more specially during the peaks  
of activity since they seem to show the biggest uncoupling between the measured parameters (del Giorgio  
& Cole 1998). Lack of total agreement regarding the statistical analysis might be related to differences in  
450 methodological sensitivity and variability. Revision of leucine (or thymidine) to carbon ratios under



different CO<sub>2</sub> levels, which might be an important source of variation between bacterial production and abundance, should be also approached to enhance our understanding in this topic.

The results from this investigation show that ocean acidification can significantly affect bacterioplankton metabolism directly by changes in the respiration rate and indirectly by changes on the organic matter with concomitant effects on bacterial production and abundance. They demonstrate that future scenarios of global change, with higher acidification might not result in a higher turnover of organic matter by bacteria.

*Acknowledgements:* This study was possible thanks to the financial support from Xunta de Galicia (7MMA013103PR project and ED431G/06 Galician Singular Research Center) and Spanish Ministry of Economy, Industry and Competitiveness (CTM2014-59345-R project and H. Sanleón-Bartolomé fellowship (FPI-IEO fellowship 2011/06)), and the technical assistance from Maria José Fernández Pazó, Vanesa Vieitez and ECIMAT staff. The authors are especially grateful to Xosé A. Alvarez-Salgado and Marta Álvarez for their scientific support and suggestions on the manuscript and to María Pérez Lorenzo and Marta Ruiz Hernández for their help with the respiration and bacterial production techniques, respectively. The authors of this study do not have conflict of interest to declare.



## 5 References:

- Allgaier M, Riebesell U, Vogt M, Thyrrhaug R, Grossart H-P (2008) Coupling of heterotrophic bacteria to phytoplankton bloom development at different pCO<sub>2</sub> levels: a mesocosm study. *Biogeosciences Discuss* 5:317–359
- Álvarez-Salgado XA, Miller AEJ (1998) Simultaneous determination of dissolved organic carbon and total dissolved nitrogen in seawater by high temperature catalytic oxidation: Conditions for precise shipboard measurements. *Mar Chem* 62:325–333
- Alvarez M, Fernandez E, Perez FF (1999) Air-sea CO<sub>2</sub> fluxes in a coastal embayment affected by upwelling: Physical versus biological control. *Oceanol Acta* 22:499–515
- Azam F, Fenchel T, Field JG, Gray JS, Meyer-Reil LA, Thingstad F (1983) The Ecological Role of Water-Column Microbes in the Sea. *Mar Ecol Prog Ser* 10:257–263
- Azam F, Grossart LBFH, Long RA, San C, La D, California J (1998) Microbial loop : its significance in oceanic productivity and global change. *Rapp Comm Int Mer Mediterr* 35:2–3
- Barcelos e Ramos J, Biswas H, Schulz KG, LaRoche J, Riebesell U (2007) Effect of rising atmospheric carbon dioxide on the marine nitrogen fixer *Trichodesmium*. *Global Biogeochem Cycles* 21:1–6
- Bunse C, Lundin D, Karlsson CMG, Vila-Costa M and 11 co-authors more (2016) Response of marine bacterioplankton pH homeostasis gene expression to elevated CO<sub>2</sub>. *Nat Clim Chang* 6:483
- Burke EJ, Brown SJ, Christidis N, Eastham J and 19 co-authors more (2014) Looking ahead in world food and agriculture: Perspectives to 2050.
- Caldeira K, Wickett ME (2008) Anthropogenic carbon and ocean pH. *Nature* 425:2100–2100
- Carrillo P, Medina-Sánchez JM, Villar-Argaiz M (2002) The interaction of phytoplankton and bacteria





in a high mountain lake: Importance of the spectral composition of solar radiation. *Limnol Ocean*  
47:1294–1306

490 Coffin RB, Montgomery MT, Boyd TJ, Masutani SM (2004) Influence of ocean CO<sub>2</sub> sequestration on  
bacterial production. *Energy* 29:1511–1520

Cole J, Findlay S, Pace M (1988) Bacterial production in fresh and saltwater ecosystems: a cross-system  
overview. *Mar Ecol Prog Ser* 43:1–10

495 Dickson AG, Goyet C (1994) Handbook of Methods for the Analysis of the Various Parameters of the  
Carbon Dioxide System in Sea Water . Edited by. *Handb methods Anal Var Param carbon dioxide*  
Syst sea water version 2 1994

Dore JE, Lukas R, Sadler DW, Church MJ, Karl DM (2009) Physical and biogeochemical modulation of  
ocean acidification in the central North Pacific. *Proc Natl Acad Sci U S A* 106:12235–40

500 Doval MD, Álvarez-Salgado XA, Pérez FF (1997) Dissolved organic matter in a temperate embayment  
affected by coastal upwelling. *Mar Ecol Prog Ser* 157:21–37

Endres S, Galgani L, Riebesell U, Schulz KG, Engel A (2014) Stimulated bacterial growth under elevated  
pCO<sub>2</sub>: Results from an off-shore mesocosm study. *PLoS One* 9:1–8

Engel A (2002) Direct Relationship between CO<sub>2</sub> Uptake and Transparent Exopolymer Particles  
Production in Natural Phytoplankton. *J Plankton Res* 24:49–53

505 Engel A, Delille B, Jacquet S, Riebesell U, Rochelle-Newall E, Terbrüggen A, Zondervan I (2004)  
Transparent exopolymer particles and dissolved organic carbon production by *Emiliania huxleyi*  
exposed to different CO<sub>2</sub> concentrations: A mesocosm experiment. *Aquat Microb Ecol* 34:93–104

Engel A, Piontek J, Grossart HP, Riebesell U, Schulz KG, Sperling M (2014) Impact of CO<sub>2</sub> enrichment



- on organic matter dynamics during nutrient induced coastal phytoplankton blooms. *J Plankton Res*  
510 36:641–657
- Fabry VJ, Seibel BA, Feely RA, Orr JC (2008) Impacts of ocean acidification on marine fauna and  
ecosystem processes. *ICES J Mar Sci* 65:414–432
- Farooq Azam and Francesca Malfatti (2007) Microbial structuring of marine ecosystems. *Nat Rev*  
*Microbiol* 5:782–791
- 515 Fraga F (1981) Upwelling off the Galician Coast, Northwest Spain. In: *Coastal Upwelling*. American  
Geophysical Union, p 176–182
- Fu FX, Warner ME, Zhang Y, Feng Y, Hutchins DA (2007) Effects of increased temperature and CO<sub>2</sub> on  
photosynthesis, growth, and elemental ratios in marine *Synechococcus* and *Prochlorococcus*  
(Cyanobacteria). *J Phycol* 43:485–496
- 520 Fuentes-Lema A, Sobrino C (2010) Efecto del incremento de CO<sub>2</sub> sobre la abundancia y biomasa del  
microfitoplancton y nanoplancton de la Ría de Vigo. *Algas* 44:2–10
- Fuentes-Lema A, Sobrino C, González N, Estrada M, Neale P (2015) Effect of solar UVR on the  
production of particulate and dissolved organic carbon from phytoplankton assemblages in the  
Indian Ocean. *Mar Ecol Prog Ser* 535:47–61
- 525 Gago J, Gilcoto M, Pérez F., Ríos A. (2003) Short-term variability of fCO<sub>2</sub> in seawater and air-sea CO<sub>2</sub>  
fluxes in a coastal upwelling system (Ría de Vigo, NW Spain). *Mar Chem* 80:247–264
- Gao K, EW H, DP H (2012) Responses of marine primary producers to interactions between ocean  
acidification, solar radiation, and warming . *Mar Ecol Prog Ser* 470:167–189
- Gasol J, Arístegui J (2007) Cytometric evidence reconciling the toxicity and usefulness of CTC as a



- 530 marker of bacterial activity. *Aquat Microb Ecol* 46:71–83
- Giorgio PA del, Cole JJ (1998) Bacterial growth efficiency in natural aquatic systems. *Annu Rev Ecol Syst* 29:503–541
- Grear JS, Rynearson TA, Montalbano AL, Govenar B, Menden-Deuer S (2017) pCO<sub>2</sub> effects on species composition and growth of an estuarine phytoplankton community. *Estuar Coast Shelf Sci* 190:40–
- 535 49
- Grossart H, Fischerhuetten A, Allgaier M, Passow U (2006) Testing the effect of CO<sub>2</sub> concentration on the dynamics of marine heterotrophic bacterioplankton. *51:1–11*
- Hein M, Sand-Jensen K (1997) CO<sub>2</sub> increases oceanic primary production Structural biology and phylogenetic estimation. *Nature* 388:526–527
- 540 Helbling EW, Carrillo P, Medina-Sánchez JM, Durán C, Herrera G, Villar-Argaiz M, Villafañe VE (2013) Interactive effects of vertical mixing, nutrients and ultraviolet radiation: In situ photosynthetic responses of phytoplankton from high mountain lakes in Southern Europe. *Biogeosciences* 10:1037–1050
- Iglesias-Rodriguez MD, Halloran PR, Rickaby REM, Hall IR, Colmenero-Hidalgo E, Gittins JR, Green
- 545 DRH, Tyrrell T, Gibbs SJ, Dassow P von, Rehm E, Armbrust EV, Boessenkool KP (2008) Phytoplankton Calcification in a High-CO<sub>2</sub> World. *Science* (80- ) 320:336–340
- Joint I, Doney SC, Karl DM (2011) Will ocean acidification affect marine microbes? *ISME J* 5:1–7
- Kroeker KJ, Kordas RL, Crim R, Hendriks IE, Ramajo L, Singh GS, Duarte CM, Gattuso JP (2013) Impacts of ocean acidification on marine organisms: Quantifying sensitivities and interaction with
- 550 warming. *Glob Chang Biol* 19:1884–1896



Langdon C, Broecker WS, Hammond DE, Glenn E, Fitzsimmons K, Nelson SG, Peng T-H, Hajdas I,  
Bonani G (2003) Effect of elevated CO<sub>2</sub> on the community metabolism of an experimental coral  
reef. *Global Biogeochem Cycles* 17:n/a-n/a

555 Lechtenfeld OJ, Hertkorn N, Shen Y, Witt M, Benner R (2015) Marine sequestration of carbon in bacterial  
metabolites. *Nat Commun* 6:6711

Levitan O, Rosenberg G, Setlik I, Setlikova E, Grigel J, Klepetar J, Prasil O, Berman-Frank I (2007)  
Elevated CO<sub>2</sub> enhances nitrogen fixation and growth in the marine cyanobacterium *Trichodesmium*.  
*Glob Chang Biol* 13:531–538

560 Liu J, Weinbauer MG, Maier C, Dai M, Gattuso JP (2010) Effect of ocean acidification on microbial  
diversity and on microbe-driven biogeochemistry and ecosystem functioning. *Aquat Microb Ecol*  
61:291–305

Moran MA, Zepp RG (1997) Role of Photoreactions in the Formation of Biologically Labile Compounds  
from Dissolved Organic Matter. *Limnol Oceanogr* 42:1307–1316

565 Motegi C, Tanaka T, Piontek J, Brussaard CPD, Gattuso JP, Weinbauer MG (2013) Effect of CO<sub>2</sub>  
enrichment on bacterial metabolism in an Arctic fjord. *Biogeosciences* 10:3285–3296

Nagata T, Fukuda H, Fukuda R, Koike I (2000) Bacterioplankton distribution and production in deep  
Pacific waters: Large-scale geographic variations and possible coupling with sinking particle fluxes.  
*Limnol Oceanogr* 45:426–435

570 Newbold LK, Oliver AE, Booth T, Tiwari B, Desantis T, Maguire M, Andersen G, Gast CJ van der,  
Whiteley AS (2012) The response of marine picoplankton to ocean acidification. *Environ Microbiol*  
14:2293–2307



- Nieto-Cid M, Álvarez-Salgado XA, Gago J, Pérez FF (2005) DOM fluorescence, a tracer for biogeochemical processes in a coastal upwelling system (NW Iberian Peninsula). *Mar Ecol Prog Ser* 297:33–50
- 575 Piontek J, Borchard C, Sperling M, Schulz KG, Riebesell U, Engel A (2013) Response of bacterioplankton activity in an Arctic fjord system to elevated pCO<sub>2</sub>: Results from a mesocosm perturbation study. *Biogeosciences* 10:297–314
- Piontek J, Lunau M, Handel N, Borchard C, Wurst M, Engel A (2010) Acidification increases microbial polysaccharide degradation in the ocean. *Biogeosciences* 7:1615–1624
- 580 Pukate Y, Rim-Rukeh A (2008) Variability with depth of some physico-chemical and biological parameters of Atlantic Ocean water in part of the coastal area of Nigeria. *J Appl Env Manag* 12:87–91
- Quere C Le, Moriarty R, Andrew RM, Peters GP and 58 co-authors more (2015) Global carbon budget 2014. *Earth Syst Sci Data* 7:47–85
- 585 Reul A, Muñoz M, Bautista B, Neale P, Sobrino C, Mercado J, Segovia M, Salles S, Kulk G, León P, Poll W van de, Pérez E, Buma A, Blanco J (2014) Effect of CO<sub>2</sub>, nutrients and light on coastal plankton. III. Trophic cascade, size structure and composition. *Aquat Biol* 22:59–76
- Riebesell U, Schulz KG, Bellerby RGJ, Botros M, Fritsche P, Meyerhöfer M, Neill C, Nondal G, Oschlies a, Wohlers J, Zöllner E (2007) Enhanced biological carbon consumption in a high CO<sub>2</sub> ocean. *Nature* 590 450:545–548
- Rochelle-Newall E, Delille B, Frankignoulle M, Gattuso JP, Jacquet S, Riebesell U, Terbruggen A, Zondervan I (2004) Chromophoric dissolved organic matter in experimental mesocosms maintained



under different pCO<sub>2</sub> levels. *Mar Ecol Prog Ser* 272:25–31

Rost B, Zondervan I, Wolf-Gladrow D (2008) Sensitivity of phytoplankton to future changes in ocean  
595 carbonate chemistry: Current knowledge, contradictions and research directions. *Mar Ecol Prog Ser*  
373:227–237

Sabine CL, Feely RA, Gruber N, Key RM and 11 co-authors more (2004) The Oceanic Sink for  
Anthropogenic CO<sub>2</sub>. *Science* (80- ) 305:367 LP-371

Sala MM, Aparicio FL, Balagué V, Boras JA and 18 co-authors more (2016) Contrasting effects of ocean  
600 acidification on the microbial food web under different trophic conditions. *ICES J Mar Sci J du Cons*  
73:670–679

Serret P, Fernández E, Sostres JA, Anadón R (1999) Seasonal compensation of microbial production and  
respiration in a temperate sea. *Mar Ecol Prog Ser* 187:43–57

Sieracki ME, Cucci TL, Nicinski J (1999) Flow cytometric analysis of 5-cyano-2,3-ditolyl tetrazolium  
605 chloride activity of marine bacterioplankton in dilution cultures. *Appl Envir Microbiol* 65:2409–  
2417

Simon M, Azam F (1989) Protein content and protein synthesis rates of planktonic marine bacteria. *Mar*  
*Ecol Prog Ser* 51:201–2013

Smith DC, Azam F (1992) A simple, economical method for measuring bacterial protein synthesis rates  
610 in seawater using tritiated-leucine. *Mar Microb Food Webs* 6:107–114

Sobrino C, Neale PJ, Phillips-kress JD, Moeller RE, Porter JA (2009) Elevated CO<sub>2</sub> increases sensitivity  
to ultraviolet radiation in lacustrine phytoplankton assemblages. 54:2448–2459

Sobrino C, Segovia M, Neale PJ, Mercado JM, García-Gómez C, Kulk G, Lorenzo MR, Camarena T,



Van de Poll WH, Spilling K, Ruan Z (2014) Effect of CO<sub>2</sub>, nutrients and light on coastal plankton.

615 IV. Physiological responses . *Aquat Biol* 22:77–93

Sobrino C, Ward ML, Neale PJ (2008) Acclimation to elevated carbon dioxide and ultraviolet radiation in the diatom *Thalassiosira pseudonana*: effects on growth, photosynthesis, and spectral sensitivity of photoinhibition. *Limnol Oceanogr* 53:494–505

Spilling K, Schulz KG, Paul AJ, Boxhammer T, Achterberg EP, Hornick T, Lischka S, Stuhr A, Bermúdez  
620 R, Czerny J, Crawford K, Brussaard CPD, Grossart H-P, Riebesell U (2016) Effects of ocean acidification on pelagic carbon fluxes in a mesocosm experiment. *Biogeosciences* 13:6081–6093

Steen AD, Arnosti C (2011) Long lifetimes of B-glucosidase, leucine aminopeptidase, and phosphatase in Arctic seawater. *Mar Chem* 123:127–132

Teira E, Fernández A, Álvarez-Salgado XA, García-Martín EE, Serret P, Sobrino C (2012) Response of  
625 two marine bacterial isolates to high CO<sub>2</sub> concentration. *Mar Ecol Prog Ser* 453:27–36

Tilstone G, Míguez B, Figueiras F, Fermín E (2000) Diatom dynamics in a coastal ecosystem affected by upwelling: coupling between species succession, circulation and biogeochemical processes. *Mar Ecol Prog Ser* 205:23–41

Yamada N, Suzumura M (2010) Effects of seawater acidification on hydrolytic enzyme activities. *J*  
630 *Oceanogr* 66:233–241

Zark M, Riebesell U, Dittmar T (2015) Effects of ocean acidification on marine dissolved organic matter are not detectable over the succession of phytoplankton blooms. *Sci Adv* 1:e1500531–e1500531

Zeebe RERE, Wolf-Gladrow DA (2001) CO<sub>2</sub> in seawater: equilibrium, kinetics, isotopes. Elsevier  
*Oceanogr Ser* 65:346



635 Table 1: Phytoplankton abundance (cells mL<sup>-1</sup>) measured by flow cytometry from phase 1 incubation aimed to obtain the organic matter inocula under acidified and non-acidified conditions.

<b>Phytoplankton abundance (cells mL<sup>-1</sup>)</b>				
	Region 1		Region 2	
	HC	LC	HC	LC
Day 2	10968 ± 4313	6207 ± 1524	1683 ± 1011	1857 ± 599
Day 5	833 ± 771	431 ± 43	1780 ± 1303	1227 ± 562
Day 7	994 ± 151	1308 ± 500	4002 ± 1913	4790 ± 333





## 6 Figure legends:

640 Figure 1. Geographical location of Ría de Vigo in the NW Iberian Peninsula. The insert shows a more detailed map of the Ría de Vigo and the locations of A) ECIMAT and B) sampling station.

Figure 2. Experimental design of the study.

645 Figure 3. A) Phytoplankton biomass measured as Chl *a* concentration and  $p\text{CO}_2$  evolution along the first incubation period aimed to obtain the organic matter inocula under current and future  $\text{CO}_2$  conditions. Black and striped vertical bars correspond to the Chl *a* mean  $\pm$  SD ( $n=3$ ) ( $\text{mg L}^{-1}$ ) obtained under high and low carbon (HC and LC) treatments, respectively. Black and grey circles correspond to the  $p\text{CO}_2$  mean  $\pm$  SD ( $n=3$ ) (ppm) in HC and LC treatments, respectively. B) Temporal evolution of the dissolved organic carbon (DOC) concentration ( $\mu\text{M} - \text{C}$ ) during this first incubation. The black and grey dots indicate the mean  $\pm$  SD ( $n=3$ ) of DOC from HC and LC treatments, respectively

650

Figure 4. Primary production measured as the incorporation of  $^{14}\text{C}$  into organic compounds during the first incubation period aimed to obtain the organic matter inocula under current and future  $\text{CO}_2$  conditions

655 A) Total organic carbon obtained from a sample independently of POC and DOC sample processing (TOC) B) Particulate organic carbon (POC) C) Dissolved organic carbon from phytoplankton origin (DOCp). Mean  $\pm$  SD ( $n=3$ ).



660 Figure 5. A)  $p\text{CO}_2$  (ppm) and B) pH values in the four treatments of the second incubation period, respectively. Mean  $\pm$  SD ( $n=3$ ). C) Temporal evolution of bacterial respiration ( $\mu\text{mol O}_2 \text{d}^{-1}$ ) in the four treatments during the second incubation period, mean  $\pm$  SD ( $n=3$ ). In all figures, black and grey triangles represent HC\_NO and HC\_AO treatments, respectively. Black and grey circles correspond to LC\_NO and LC\_AO treatments.

665 Figure 6. Bacterial viability (Viable bacterial  $\text{mL}^{-1}$ ) measured with the CTC dye on day 7, mean  $\pm$  SD ( $n=3$ ). The asterisk indicate mean significant difference with the other treatments with  $p\text{-value} < 0.05$ .

670 Figure 7. Temporal evolution of the dissolved organic carbon (DOC) concentration ( $\mu\text{M} - \text{C}$ ) during the second incubation period. Black and grey triangles represent HC\_NO and HC\_AO treatments, respectively. Black and grey circles correspond to LC\_NO and LC\_AO treatments, respectively. The two asterisks indicate significant differences between LC vs. HC treatments with  $p\text{-value} < 0.01$ .

675 Figure 8. A) Histogram of bacterial abundance evolution ( $\text{Cells mL}^{-1}$ ) in the four treatments during the course of the second incubation period, mean  $\pm$  SD ( $n=3$ ). Treatments with different letter indicate significant differences ( $p\text{-value} < 0.05$ ). B) Bacterial production ( $\mu\text{g C L}^{-1} \text{d}^{-1}$ ) from the four treatments during the second incubation period, mean  $\pm$  SD ( $n=6$ ). Asterisks indicate significant differences between NO vs. AO treatments with  $p\text{-value} < 0.05$ . Black and grey triangles represent HC\_NO and HC\_AO treatments, respectively. Black and grey circles correspond to LC\_NO and LC\_AO treatments, respectively.



680

Figure 9. A) Bacterial carbon demand (BCD) and B) Bacterial growth efficiency (BGE) calculated from the bacterial production and respiration rates obtained from this study. Asterisks indicate significant differences with  $p$ -value  $< 0.05$  between NO vs. AO treatments, for the BCD and between HC\_NO vs. the rest of the treatments (LC\_NO, LC\_AO and HC\_AO) for the BGE. Black and grey triangles represent 685 HC\_NO and HC\_AO treatments, respectively. Black and grey circles correspond to LC\_NO and LC\_AO treatments, respectively.



FIGURE 1:

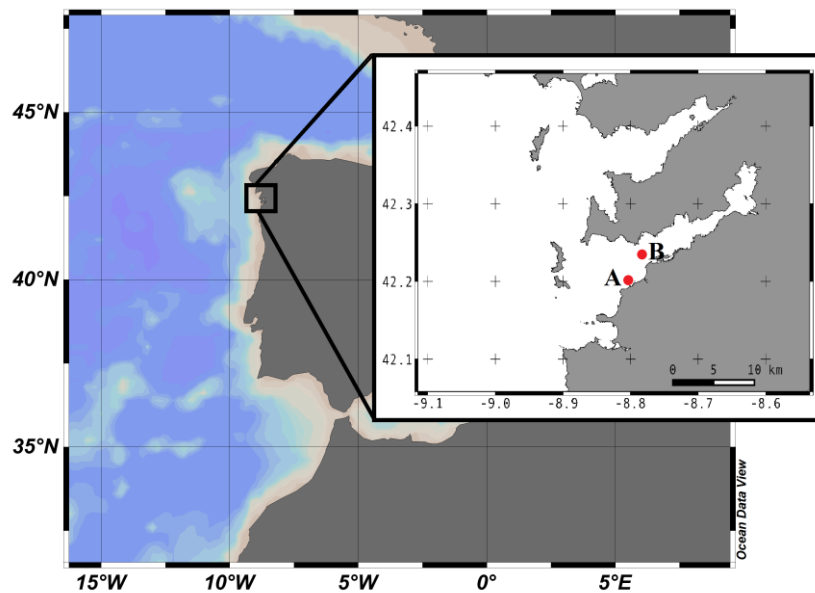




FIGURE 2:

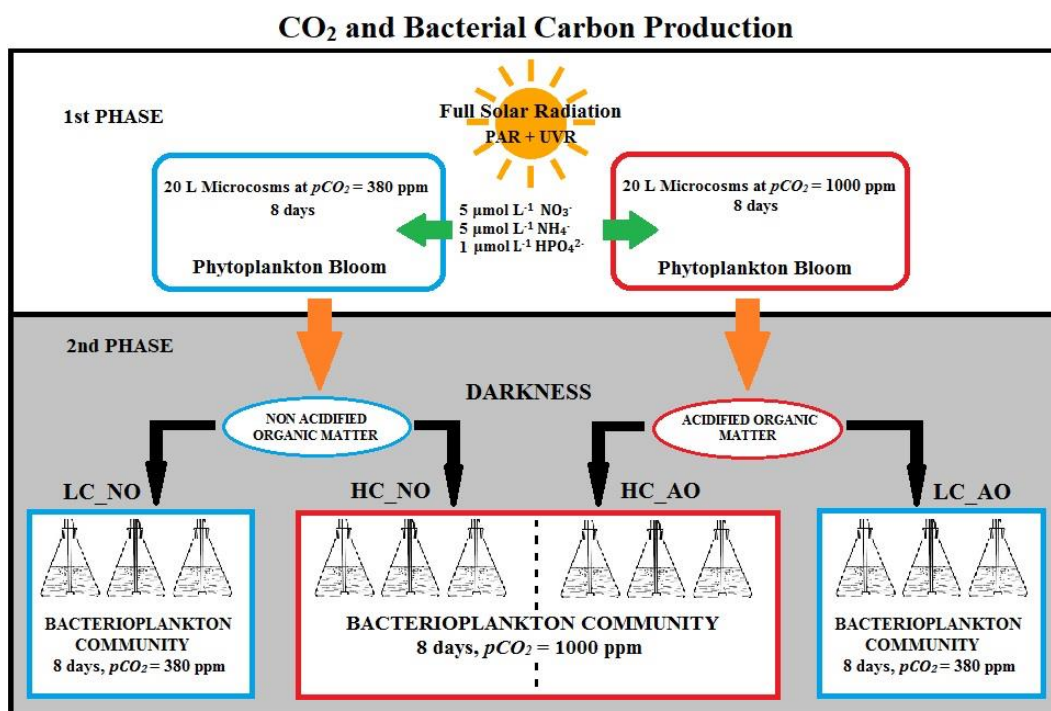
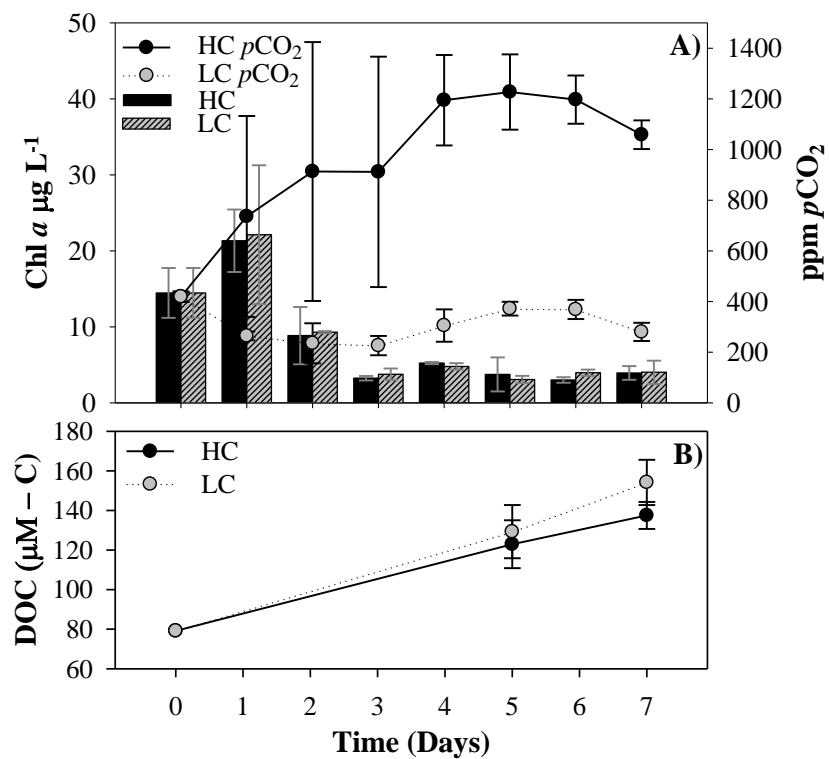




FIGURE 3:





690 FIGURE 4.

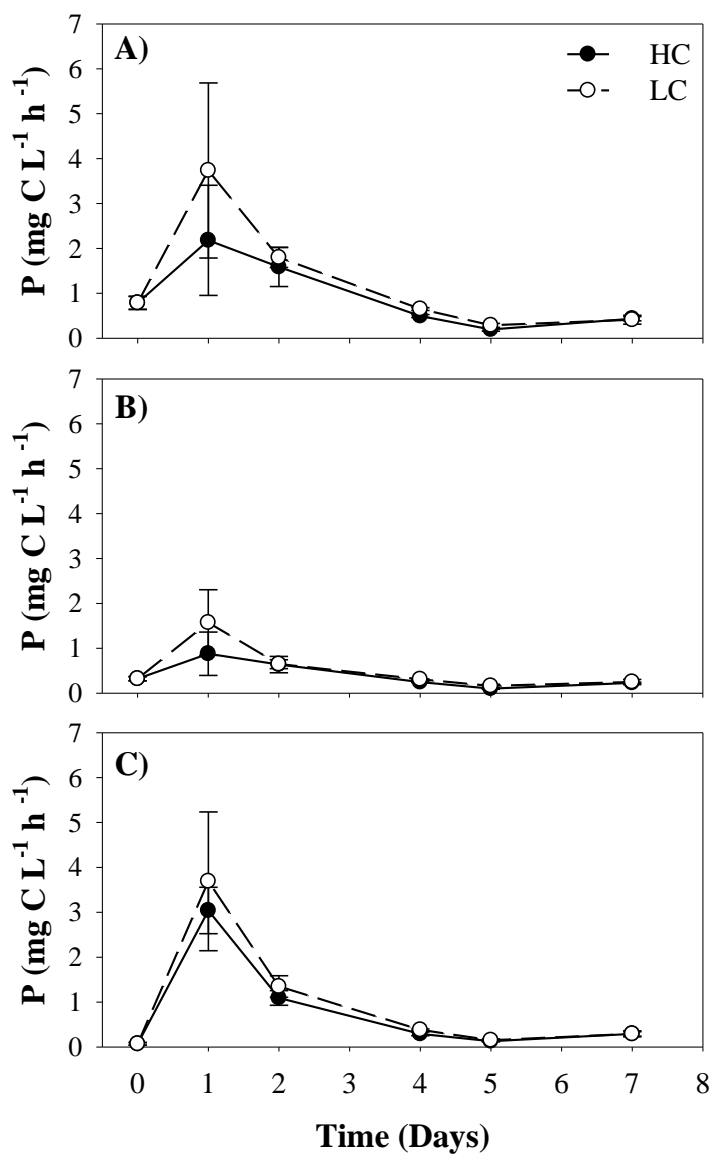




FIGURE 5:

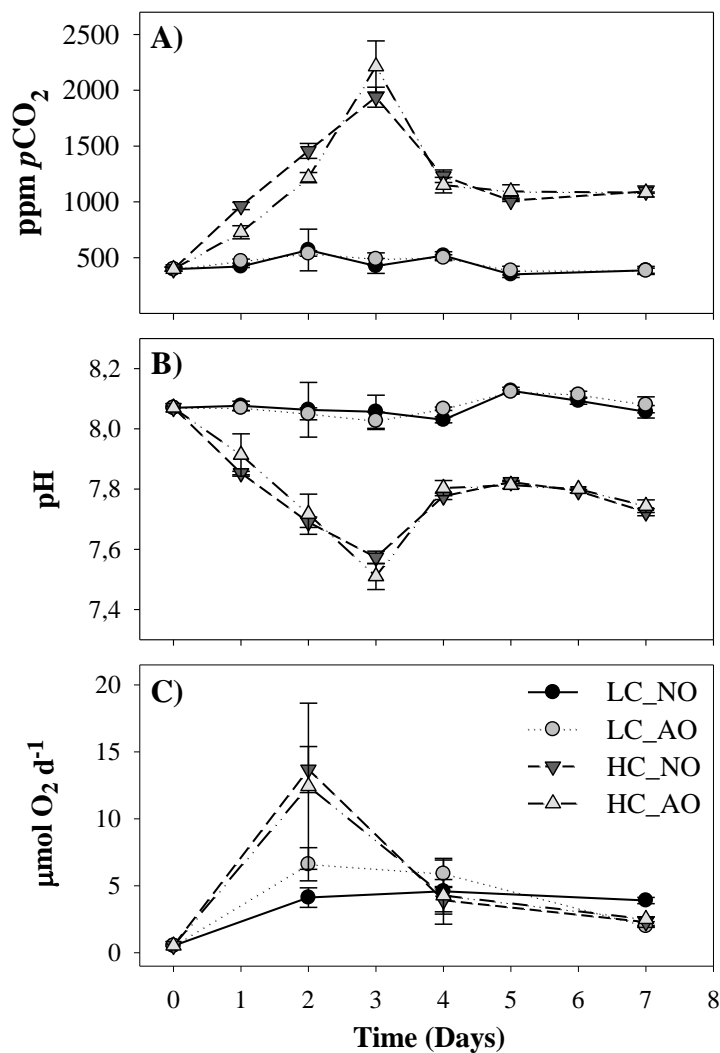






FIGURE 6:

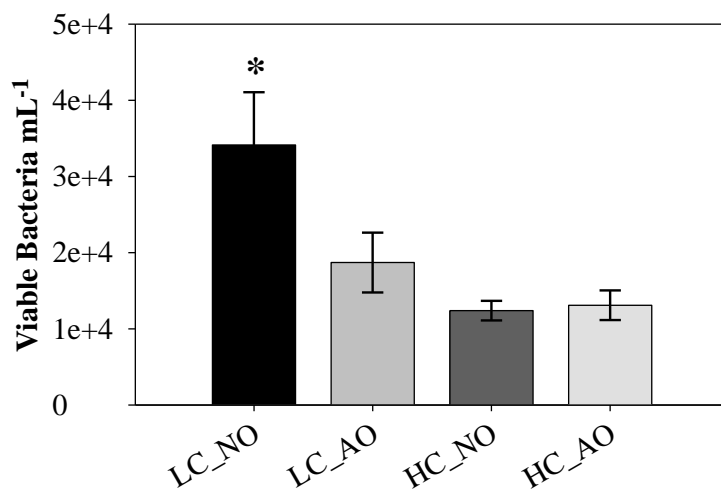




FIGURE 7:

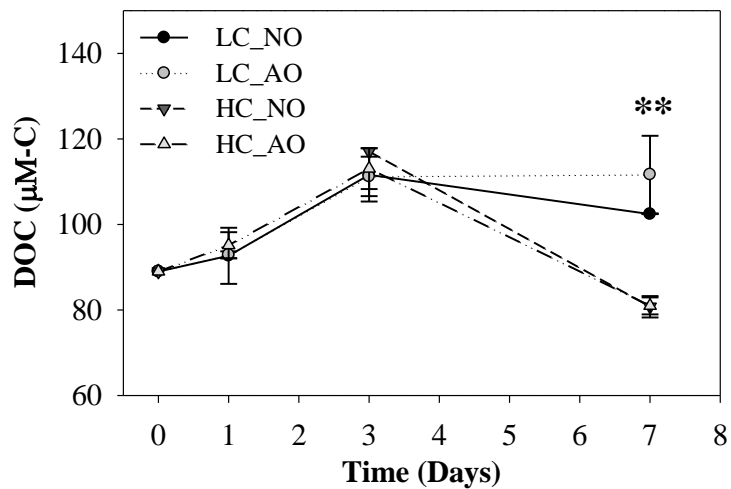
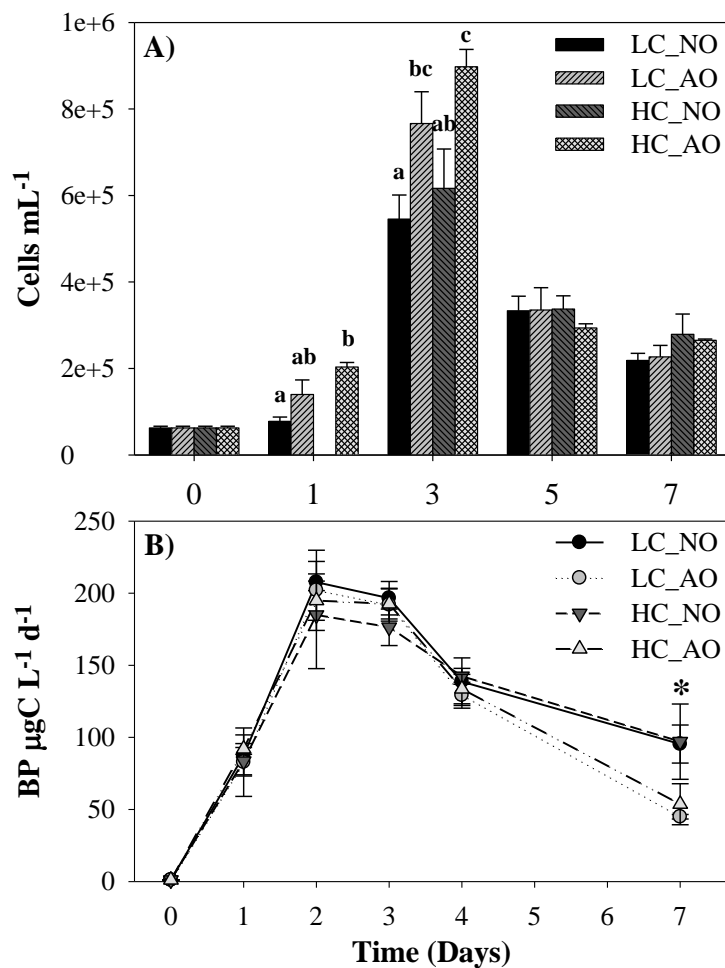




FIGURE 8:





695 FIGURE 9:

